Cell. Mol. Life Sci. 64 (2007) 487 – 497
1420-682X/07/040487-11
DOI 10.1007/s00018-007-6427-1

Cellular and Molecular Life Sciences

Research Article

Effects of ulapualide A and synthetic macrolide analogues on actin dynamics and gene regulation

E. Vincent[a, +, †], J. Saxton[a, †], C. Baker-Glenn[b], I. Moal[b], J. D. Hirst[b], G. Pattenden[b] and P. E. Shaw[a, *]

[a] Centre for Biochemistry and Cell Biology, School of Biomedical Sciences, University of Nottingham, Queen's Medical Centre, Nottingham NG7 2UH (UK), e-mail: peter.shaw@nottingham.ac.uk
[b]School of Chemistry, University Park, Nottingham NG7 2RD (UK)

Received 27 September 2006; received after revision 30 November 2006; accepted 8 January 2007
Online First 5 February 2007

Abstract. Several marine macrolide toxins act as potent and specific actin-severing molecules. Recent elucidation of their stereochemistries and modes of interaction with actin has allowed the syntheses of bioactive analogues. Here we used synthetic analogues in a structure-function analysis of ulapualide A, a trisoxazole-based macrolide. Ulapualide A harboured potent actin-depolymerising activity both in cells and *in vitro*. Its synthetic diastereoisomer was three orders of magnitude less active than the natural toxin and synthetic macrolide fragments lacked actin-capping/severing activity altogether. Modulation of serum response factor (SRF)-dependent gene expression, as described for other actin-binding toxins, was also examined. Specific changes in response to ulapualide A were not observed, primarily due to its profound effects on cytoskeletal integrity and cell adhesion. Several synthetic fragments of ulapualide A also had no effect on SRF-dependent gene expression. However, inhibition was observed with a molecule corresponding to the extended aliphatic side chain of halichondramide, a structurally related macrolide. These findings indicate that side-chain derivatives of trisoxazole-based macrolides may serve to uncouple gene-regulatory events from actin dynamics.

Keywords. Actin cytoskeleton, immediate early genes, toxins, transcription, serum response factor.

Introduction

The cytotoxic effects of numerous marine macrolides hinge on their ability to disrupt actin dynamics [1, 2], which in turn underlie numerous cellular processes including cell adhesion, migration, trafficking, signal transduction and gene regulation (for reviews see [3, 4]). Interest in these drugs has been enhanced by the perception of the cytoskeleton as a promising target for therapeutic intervention [5]. Actin filaments (F-actin) are highly dynamic components of the cytoskeleton, polymerising from actin monomers (G-actin) at the + end and depolymerising at the – end. The process is regulated by the reciprocal action of actin-capping molecules such as CapZ, which stabilise F-actin, and actin-severing molecules such as gelsolin and cofilin. In addition, polymerisation is promoted by factors such as profilin, which binds to G-actin [4].
In recent years, actin dynamics have also been shown to regulate a subset of genes containing serum response elements (SREs) through the titration of transcription factors belonging to the Myocardin family by G-actin [6–8]. Depletion of the cytoplasmic

[+] Present address: Department of Biochemistry, University of Bristol, Bristol BS8 1TD (UK)
[†] These two authors contributed equally
[*] Corresponding author.

G-actin pool allows MAL/MKL-1 to reach the nucleus, where it interacts with serum response factor (SRF) at target gene promoters. Several drugs that perturb actin dynamics, such as latrunculin B, jasplakinolide, swinholide A and cytochalasin D [9–12] modulate these events [8, 13].

Crystal structures of the complexes between G-actin and several trisoxazole-based macrolides have been reported recently [14, 15]. Kabiramide C and jaspisamide A bind with G-actin in what was proposed to be a two-step interaction, whereby the macrocyclic ring of the natural product first interacts with a hydrophobic patch at the interface between sub-domains 1 and 3 of actin, followed by insertion of the aliphatic tail into the hydrophobic cleft between the two sub-domains, making extensive hydrophobic interactions with actin [16]. In the case of ulapualide A [15], a trisoxazole-based macrolide isolated from nudibranchs (sea slugs), the trisoxazole macrocylic head made similar hydrophobic interactions with residues I341, I345, S348 and L349 of G-actin; however, the aliphatic tail lacked electron density in the crystal structure and appeared to have rotational freedom in the complex. This difference notwithstanding, kabiramide C, jaspisamide A and ulapualide A mimic the binding of gelsolin, and were all predicted to disrupt actin fibres, as demonstrated for halichondramide [1], and more recently kabiramide C, resulting in inhibition of cell motility and cytokinesis [16].

The total synthesis of ulapualide A has been achieved [17, 18], although the synthetic compound was a diastereoisomer, differing at five chiral centres from the natural product [15]. For this reason the synthetic diastereoisomer was presumed to lack biological function. However, as the biological activity of ulapualide A had not been examined in detail, we decided to compare directly the activities of the natural and synthetic macrolides. In addition, the availability of synthetic compounds corresponding to fragments of trisoxazole macrolides afforded the opportunity to perform a structure-function analysis, which could potentially serve to test hypotheses made from the crystal structures about their mode of action as filament-severing and actin-capping molecules [14].

Here we confirm that ulapualide A is a highly potent disruptor of the actin cytoskeleton, whereas the synthetic diastereoisomer is at least three orders of magnitude less active. Although morphological changes induced by ulapualide A resembled those of latrunculin B, which sequesters G-actin monomers but can also induce F-actin depolymerisation [2], the anticipated changes to gene regulation in response to actin depolymerisation, as seen with latrunculin B [8, 13], were not observed with ulapualide A. Instead, analysis of several synthetic fragments of ulapualide A revealed that, whereas the macrocyclic head lacked both actin-capping and gene-modulatory activity, the extended aliphatic tail inhibited SRF-dependent gene regulation.

Materials and methods

Cell culture and transfections. Human embryonal kidney (HEK293), HeLa and NIH3T3 cells were cultured in DMEM supplemented with 10% foetal calf serum (FCS) and penicillin/streptomycin. HEK293 cells were transfected by DNA-calcium phosphate co-precipitations as described previously [19]. NIH3T3 cells were transfected with polyethyleneimine (PEI) [20].

Plasmids. The SREluc3 and DSEluc3 reporter plasmids contain a single copy of the SRE/DSE upstream from the Adenovirus 2 E4 basal promoter inserted into pGL3basic. The expression plasmid for RhoA(Q63L) has been described [19].

Toxins. Ulapualide A, the synthetic diastereoisomer and partial fragments were available as solids or oils; they were dissolved in DMSO at stock concentrations of 10 mM. Latrunculin B was purchased from Sigma; cytochalasin D was from Calbiochem; rhodamine-conjugated phalloidin was from Invitrogen.

Cell adhesion assays and confocal microscopy. NIH3T3 cells or HeLa cells were incubated in DMEM/10% FCS for 2 h in a plastic tube. Medium containing toxins at various concentrations were distributed in 12-well plates and 1×10^6 cells were added to each well. After 2 h, plates were washed twice with phosphate-buffered saline (PBS). Cells were imaged with a Zeiss Axiovert 100 microscope and Axiocam digital camera and counted. For confocal microscopy cells were fixed with 4% paraformaldehyde, washed in PBS, submerged in 0.2% Triton X-100 for 3 min and washed again in PBS. Cells were then incubated in 1% BSA in PBS for 30 min prior to staining with phalloidin in methanol. Images were collected on a Zeiss LSM510 confocal system through a Plan-Apochromat 63x/1.4 oil objective and processed with Zeiss LSM software.

Actin sedimentation assay. The assay was performed essentially as previously described [21]. G-actin (24 μM) was incubated for 1 h at room temperature in polymerisation buffer (5 mM Tris-HCl pH 8, 0.2 mM ATP, 100 mM KCl, 2 mM $MgCl_2$) with or without toxin, prior to centrifugation at 100 K rpm for 15 min at 20°C in a Beckman TLA100 rotor. Pellets were re-dissolved in SDS-PAGE loading buffer and aliquots were loaded, in parallel with the corresponding supernatants, onto 10% denaturing polyacrylamide gels. After electrophoresis, gels were stained with Coomassie brilliant blue.

Reporter assays. HEK293 cells were washed 18 h post-transfection and incubated in DMEM supplemented with 0.5% FCS for 24 h in the presence of toxin. Cells were harvested in cold PBS and lysed in 250 mM KCl, 50 mM HEPES pH 7.5, 0.1% NP40, 10% glycerol. Luciferase activity was measured in a Berthold 953 luminometer and normalised against β-galactosidase activity from a co-transfected plasmid (pCH110).

Molecular modelling. The ulapualide geometry was taken from the crystallographic structure (PDB code 1S22). Some of the ulapualide atoms are not resolved; the missing atoms were taken from the corresponding atoms in kabiramide (PDB code 1QZ5), after superposition by root mean square deviation (rmsd) minimization. The geometries of the other molecules of interest were derived by modification of the ulapualide structure. Protecting groups were replaced with hydrogen atoms. The structure of actin was taken as a monomer from the dimer complexed with swinholide (PDB code 1YXQ chain A). The methylated histidine was treated as a standard histidine residue. All non-protein molecules (ethylene glycol, ATP, metal ions and crystallographic water) were excluded from the docking. The absence of crystallographic water means that experimentally observed water-mediated interactions with the N-methyl formamide moiety will not be modelled, but as the overall

intermolecular interaction of the ligands with actin is predominantly hydrophobic, this may not be too severe an omission. Docking was performed using the AutoDockTools interface to AutoDock 3.0 [22], which employs an empirical potential calculated on a grid, prior to a conformational search using a Lamarckian genetic algorithm. The atomic affinity and electrostatic potential were computed on a cubic grid of edge 41.25 Å, with a 0.375-Å probe atom separation. Bond angles and bond lengths were kept fixed. Torsion angles for bonds within a ring were not deemed rotatable. Flexibility was permitted for polar hydrogen atoms, terminal groups, atoms that were not resolved in the 1S22 PDB structure and their adjacent atoms. This amounted to 11 rotatable bonds for the larger fragments 125 and E, or as few as 4 for TRIS. The genetic algorithm search parameters were the default setting, except for the following, which were increased in view of the relatively large search space: population of 50, a maximum generation limit of 200 000 and energy evaluation limit of 1 000 000. All fragments were initially positioned within the binding site, with a random orientation and random bond angles.

Results

Ulapualide A blocks cell adhesion and disrupts morphological integrity. Initial experiments were performed to test for toxicity of ulapualide A and several related compounds (see Fig. 1) on HEK293, NIH3T3 and HeLa cells. Compounds were applied to growing cells at concentrations ranging from 0.1 nM to 10 μM and cells were observed periodically over 24 h by phase-contrast microscopy. The only compound with overt effects was ulapualide A, which caused cells to round up and detach from the plastic within 2–4 h at nanomolar concentrations (data not shown). As some cells appeared to survive the lower ulapualide A concentrations, we monitored the stability of the compound under cell culture conditions. In the absence of cells, ulapualide A retained activity well (half-life approx. 15 h), but in the presence of cells its activity decreased rapidly, most likely due to the toxin being taken up by the cells and bound by actin (data not shown).

To measure the effect of ulapualide A on cell adhesion, a settling assay was performed in which NIH3T3 cells were plated in full medium and allowed to adhere in the presence of increasing drug concentrations. After 24 h, the plates were washed and the adherent cells counted. Ulapualide A had a striking impact in this assay as it blocked cell adhesion at 10 nM, a concentration at least three orders of magnitude lower than the effective dose of latrunculin B (see Fig. 2a). None of the partial compounds had any effect in this assay, as exemplified by 125, corresponding to the aliphatic tail of halichondramide, a toxin closely related to ulapualide A. Similar results were also obtained with HeLa cells, although their sensitivity to ulapualide A was less pronounced (data not shown). In a direct comparison with ulapualide A, the synthetic diastereoisomer was only weakly active in this assay (Fig. 2b). These experiments suggest that ulapualide A potently disrupts actin dynamics and indicate that the activity of its synthetic diastereoisomer is severely compromised.

Ulapualide A disrupts the actin cytoskeleton. The effects of ulapualide A and several synthetic, partial analogues on the actin cytoskeleton were examined directly by phalloidin staining and confocal microscopy. As shown in Figure 3a, actin filaments were prominent in the lamellipodia at the periphery of proliferating NIH3T3 cells. Treatment with ulapualide A (100 nM) rapidly disrupted the integrity of the cytoskeleton and the phalloidin staining became weak, condensed and punctate. Furthermore, the cells rounded up and began to detach from the glass. Latrunculin B induced a similar response but only with a higher dose (10 μM) and over a longer period (5 h). None of these effects was seen with 125 (Fig. 3a) or any of the other partial compounds tested (data not shown). The analysis was performed on HeLa cells with identical results (data not shown). We also compared ulapualide A with its synthetic diastereoisomer in this assay (Fig. 3b). At low concentrations (100 nM) the diastereoisomer had no effect on the actin cytoskeleton but some disruption was apparent at higher concentrations (10 μM). Taken together, the data demonstrate the potency with which ulapualide A disrupts the actin cytoskeleton in comparison to its diastereoisomer and latrunculin B.

Actin-capping and -severing activity of ulapualide A. An *in vitro* sedimentation assay was used to study the direct effect of ulapualide A and its diastereoisomer on actin polymerisation. Incubation of G-actin with 100 mM KCl leads to the formation of F-actin, which can be collected by ultracentrifugation [21]. As shown in Figure 4, routinely about 80% polymerisation of the soluble G-actin (S) could be achieved, as estimated from the fraction recovered from pellets (P) (compare lanes 2 and 3 with 4 and 5 in all panels). Actin polymerisation was completely inhibited by ulapualide A at concentrations above 1 μM and was partially inhibited at 100 nM (upper panel, lanes 6–11), indicating that ulapualide A possesses potent actin capping activity. When tested in the same assay both the synthetic diastereoisomer (middle panel) and 125, the aliphatic tail of halichondramide (lower panel), were inactive.

To detect F-actin-severing activity, the experiment was repeated in modified form, whereby toxin was added post polymerisation. Ulapualide A reversed F-actin formation above 1 μM and showed a partial effect at 100 nM (Fig. 4b), indicating that it is equally potent as an F-actin-severing molecule. Given their

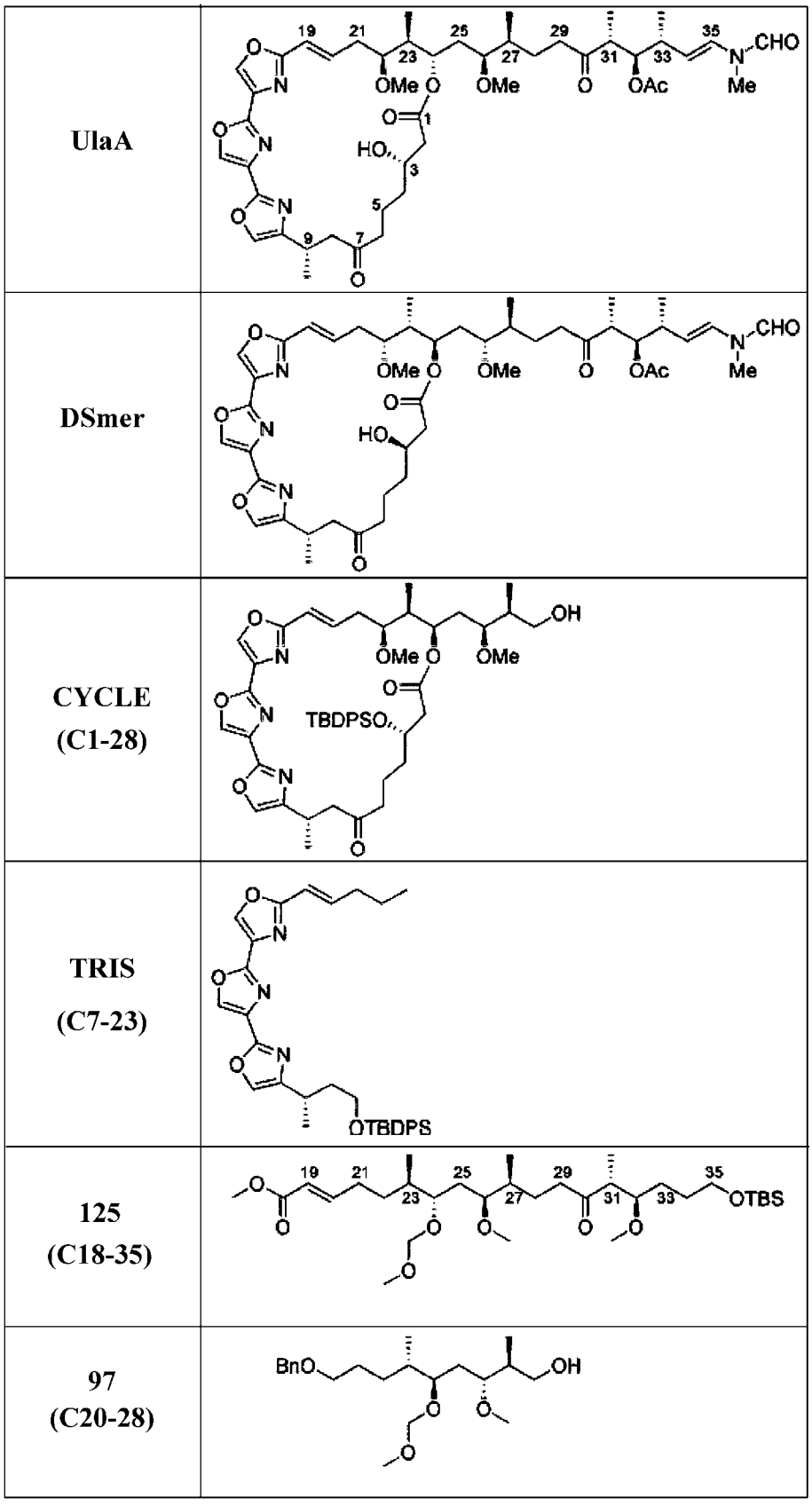

Figure 1. Structure of ulapualide A and related synthetic compounds used in this study. UlaA, ulapualide A; DSmer, synthetic diasteroisomer of ulapualide A; CYCLE (C1–28), *Tris*-oxazole macrocycle of ulapualide A; TRIS (C7-23), 4-[(S)-3-(*tert*-Butyl-diphenyl-silanyloxy)-1-methyl-propyl]-2''-[(*E*)-pent-1-enyl]-[2,4';2',4'']teroxazole; (125: C18–35) (*E*)-(6*R*,7*S*,9*S*,10*S*,14*R*,15*R*)-18-(*tert*-butyl-dimethyl-silanyloxy)-9,15-dimethoxy-7-methoxy-methoxy-6,10,14-trimethyl-13-oxo-octadec-2-enoic acid methyl ester, 97 (C20–28), (2S,3*R*,5*R*,6*S*)-9-benzyloxy-3-methoxy-5-methoxy-methoxy-2,6-dimethyl-nonan-1-ol.

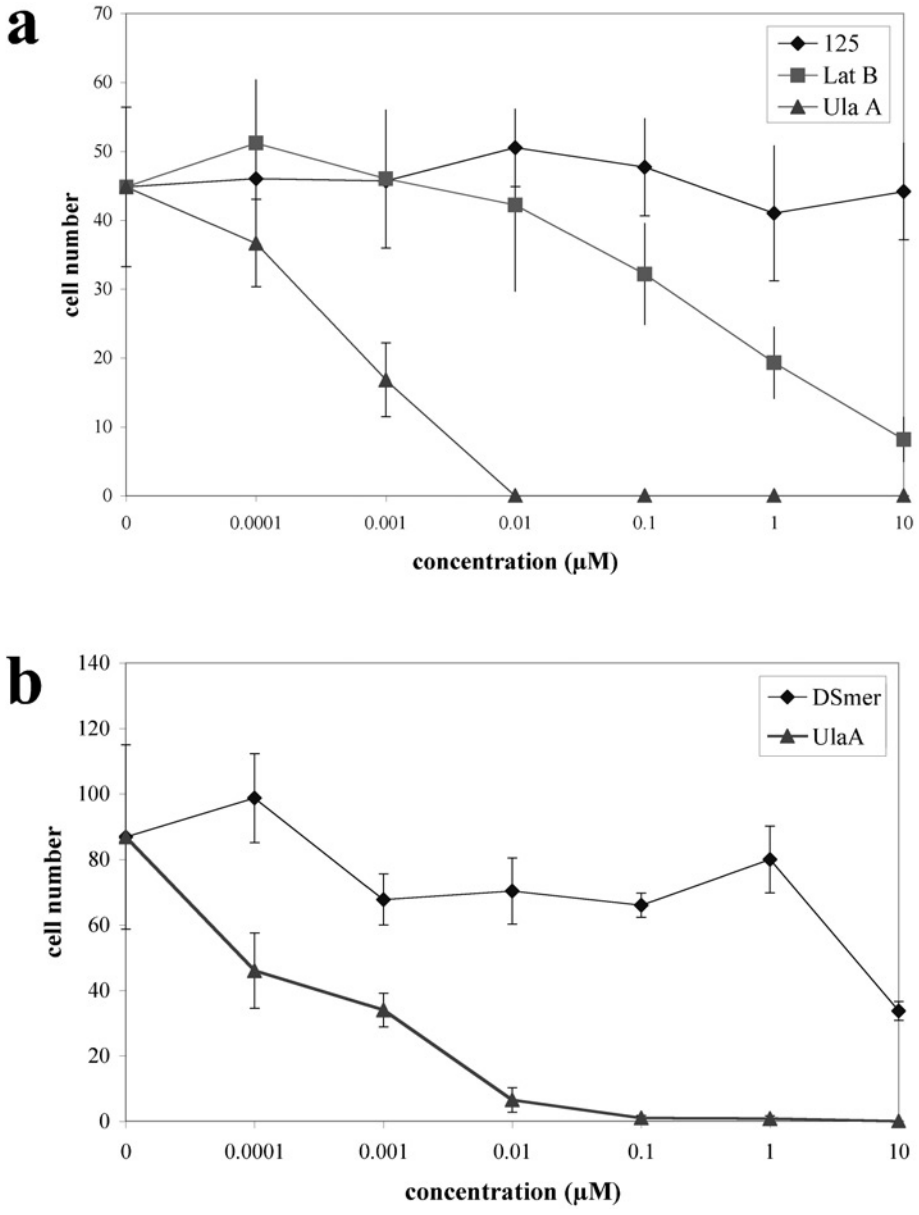

Figure 2. Effect of selected macrolides on cell adhesion. (*a*) NIH3T3 cells were plated in full medium with increasing concentrations of ulapualide A (UlaA), latrunculin B (LatB) or the synthetic tail of halichondramide (125). (*b*) NIH3T3 cells were plated in full medium with increasing concentrations of ulapualide A (UlaA), or the synthetic diastereoisomer (DSmer). Cell numbers correspond to adherent cells after 24 h per field of view (error bars represent SD, n=6).

failure to block polymerisation, the diastereoisomer and 125 were not tested in this assay. These findings indicate that ulapualide A acts as an actin-capping and -severing toxin.

Inhibition of gene expression by the aliphatic tail of halichondramide. To look for an effect of ulapualide A or the available synthetic analogues on actin-dependent gene regulation, a reporter assay similar to that established by Hill *et al.* [23] was adopted, consisting of a firefly luciferase reporter driven by a single copy of the c-*fos* SRE upstream of a basal promoter. In HEK293 cells, the activity of this reporter was elevated four- to fivefold by expression of a constitutively active RhoA protein (RhoA-Q63L), which, as anticipated, was reversed by treatment of the cells with 1 μM latrunculin B (see Fig. 5a) as reported earlier [8].

Given the effect of ulapualide A on cell adhesion, preliminary titration experiments were performed whereby cells were treated with ulapualide A at concentrations ranging from 1 μM to 0.1 nM. After 24 h, adherent cells were harvested for reporter expression analysis. Although the numbers of adherent cells decreased with increasing ulapualide A concentration, when normalised against β-galactosidase expression there was no reproducible effect of ulapualide A on basal or RhoA-activated reporter gene expression (data not shown). Thus, although the actin cytoskeleton was perturbed by nanomolar con-

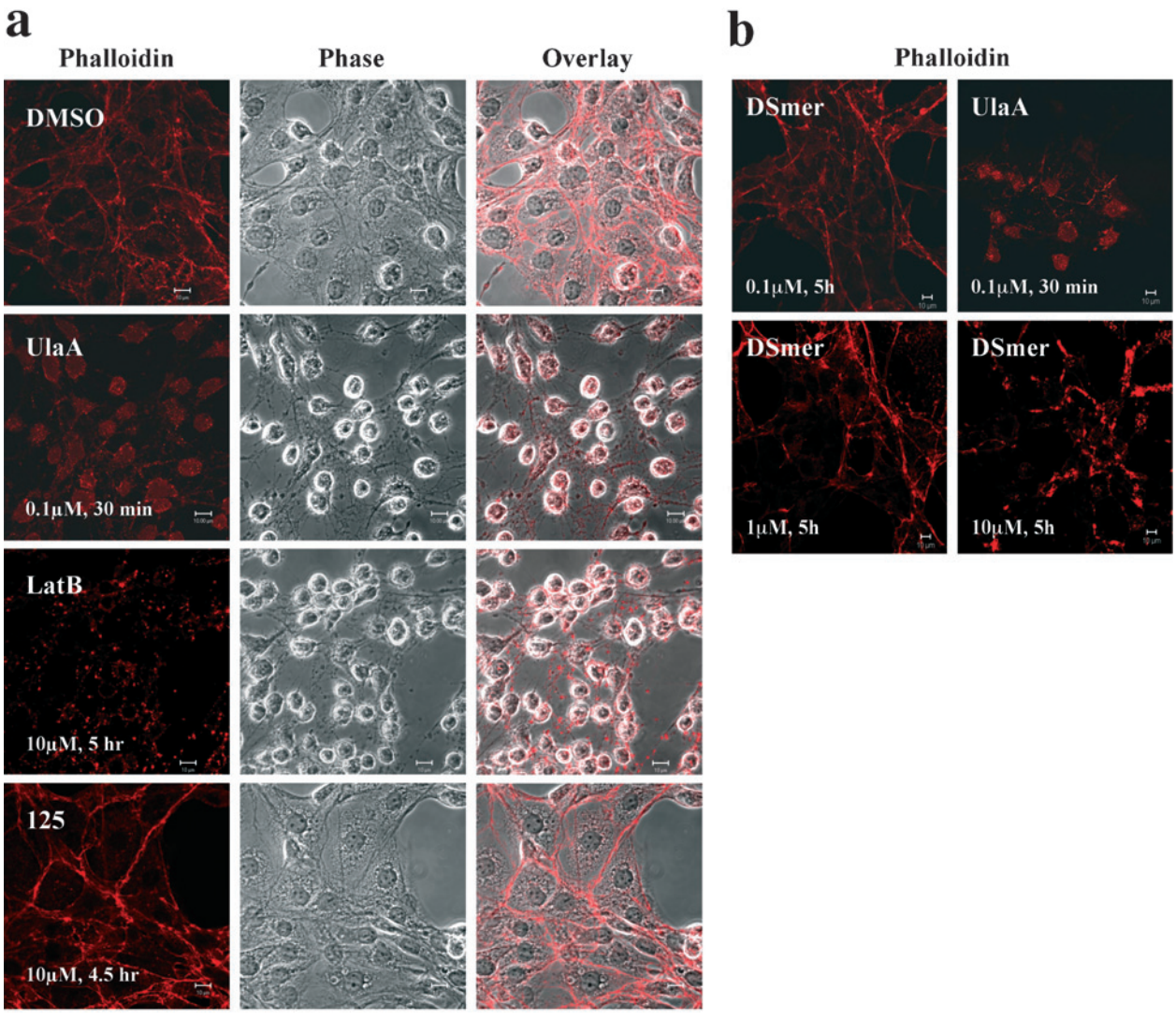

Figure 3. Effect of selected macrolides on the actin cytoskeleton. (*a*) Adherent NIH3T3 cells were treated with DMSO (vehicle) or ulapualide A (0.1 μM), latrunculin B (10 μM) or 125 (10 μM) for the times indicated. (*b*) Adherent NIH3T3 cells were treated with ulapualide A (0.1 μM), or with different concentrations of the synthetic diastereoisomer for the times indicated. Cells were fixed, stained with phalloidin and imaged by confocal microscopy.

centrations of ulapualide A (Fig. 2), a specific effect on SRE-dependent reporter expression could not be demonstrated (see also Fig. 5a).

Although none of the synthetic analogues of ulapualide A showed any effect on actin dynamics, their ability to influence SRE reporter activity was also examined (Fig. 5a). Neither the macrocyclic ring (CYCLE: C1–28) nor the trisoxazole moiety (TRIS: C7–23) influenced the SRE reporter, even at 10 μM final concentrations. In contrast, a compound corresponding to the aliphatic tail of halichondramide (125: C18–35), which differs from the tail of ulapualide A by its substituents at C23, C32 and C33 and the absence of the terminal NMeCHO moiety (see Figs 1 and 6a), inhibited RhoA-dependent SRE reporter activity completely and reproducibly ($p<0.001$; see Fig. 5c). A truncated version of the tail with somewhat altered stereochemistry (97: C20–28) was devoid of activity. Because the SRE also responds to signals transduced by MAPK pathways, which are mediated by ternary complex factors (TCFs) such as Elk-1 [3, 24, 25], these analyses were repeated with a reporter based on a mutant SRE (DSE) that binds SRF and allows the recruitment of MAL/MKL-1 but does not support the binding of Elk-1 [23]. Although the DSE showed lower activity overall, its response spectrum mirrored that of the SRE, as anticipated (Fig. 5b), consistent with the notion that RhoA-induced reporter expression was independent of the MAPK-TCF axis.

To probe further the structural requirements for this inhibitory activity, three additional compounds corresponding to parts of the aliphatic tail in ulapualide A

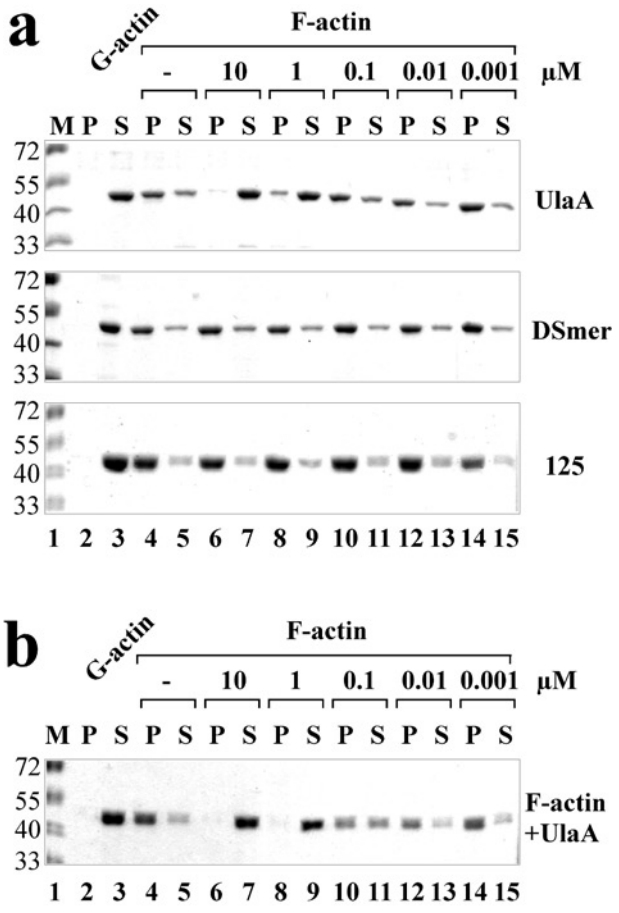

Figure 4. Effect of ulapualide A on actin polymerisation *in vitro*. (*a*) Actin was incubated for 1 h in the absence (lanes 2 and 3) or presence of 100 mM KCl (lanes 4–15) and ulapualide A (upper), diastereoisomer (middle) or compound 125 (lower panel) at 10 µM (lanes 6 and 7), 1 µM (lanes 8 and 9), 0.1 µM lanes 10 and 11), 10 nM (lanes 12 and 13) or 1 nM (lanes 14 and 15). Samples were then centrifuged and soluble (S) and pellet (P) fractions were analysed by SDS-PAGE. (*b*) As in (*a*) except that actin was allowed to polymerise for 1 h prior to incubation with ulapualide A at the concentrations indicated.

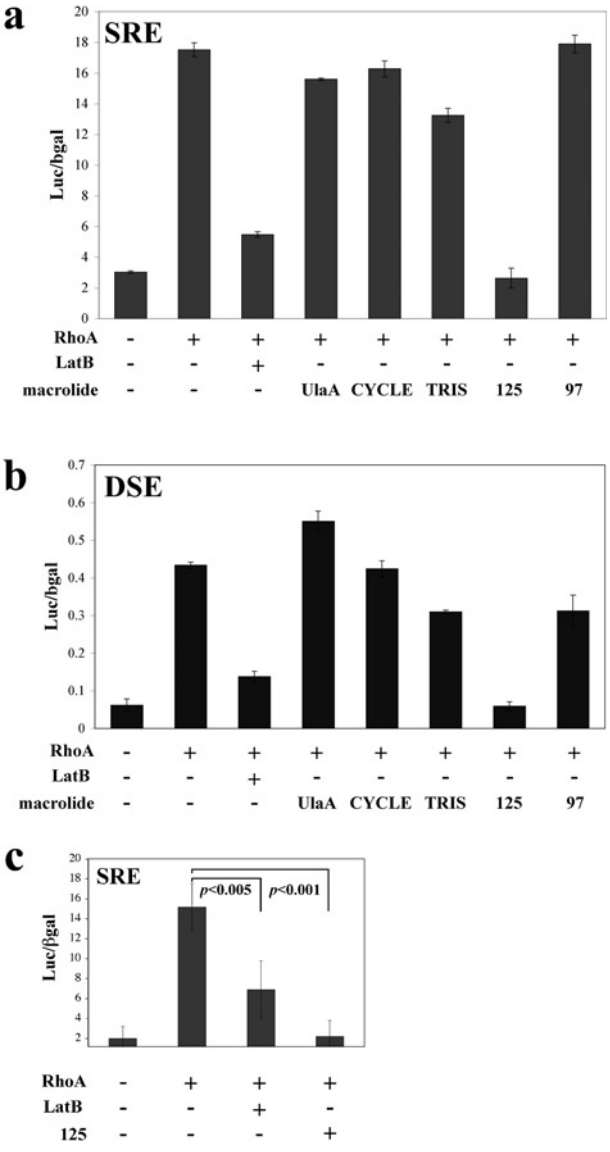

Figure 5. Effect of synthetic macrolide moieties on SRF-dependent reporter gene expression. (*a*) HEK293 cells transfected with a SRE-luciferase reporter, a control β-galactosidase plasmid and an expression plasmid for active RhoA were incubated in medium with low serum for 24 h without compound or with 1 µM latrunculin B (LatB), 0.1 µM ulapualide A (UlaA), 10 µM CYCLE, 10 µM TRIS, 10 µM 125 (C18–35) or 10 µM 97 (C20–28) as indicated (error bars represent SD, n=2). (*b*) HEK293 cells transfected with a DSE-luciferase reporter, a control β-galactosidase plasmid and an expression plasmid for active RhoA were incubated in medium with low serum for 24 h without compound or with 1 µM latrunculin B (LatB), 0.1 µM ulapualide A (UlaA), 10 µM CYCLE, 10 µM TRIS, 10 µM 125 (C18–35) or 10 µM 97 (C20–28) as indicated (error bars represent SD, n=2). (*c*) Data amalgamated from Figures 5a and 6b were analysed by a two-tailed Student's *t*-test.

were compared with 125 (C18–35) in the reporter assay; B (C20–28), which is similar to 97 but with stereochemistry corresponding to that of ulapualide A; H (C26–35), which corresponds to the tail of ulapualide A; and E (C20–35), which differs from 125 only by the truncation of the structure at C20 (see Fig. 6A). However, unlike 125, none of the compounds was able to influence SRE-dependent reporter expression (Fig. 6b) and no effects on cell adhesion were observed (not shown).

Docking studies predict that ulapualide A fragments bind G-actin. One explanation for the inhibition of SRF-dependent gene expression by 125 (C18–35) is that the isolated aliphatic tail of ulapualide A or its related macrolides might complex with G-actin. As 77% of the solvent accessible surface of non-polar atoms in the aliphatic tail of kabiramide C was calculated to be in contact with actin [14], flexible docking studies were performed with the AutoDock programme [22] to explore this possibility theoretically (see Materials and methods). With this algo-

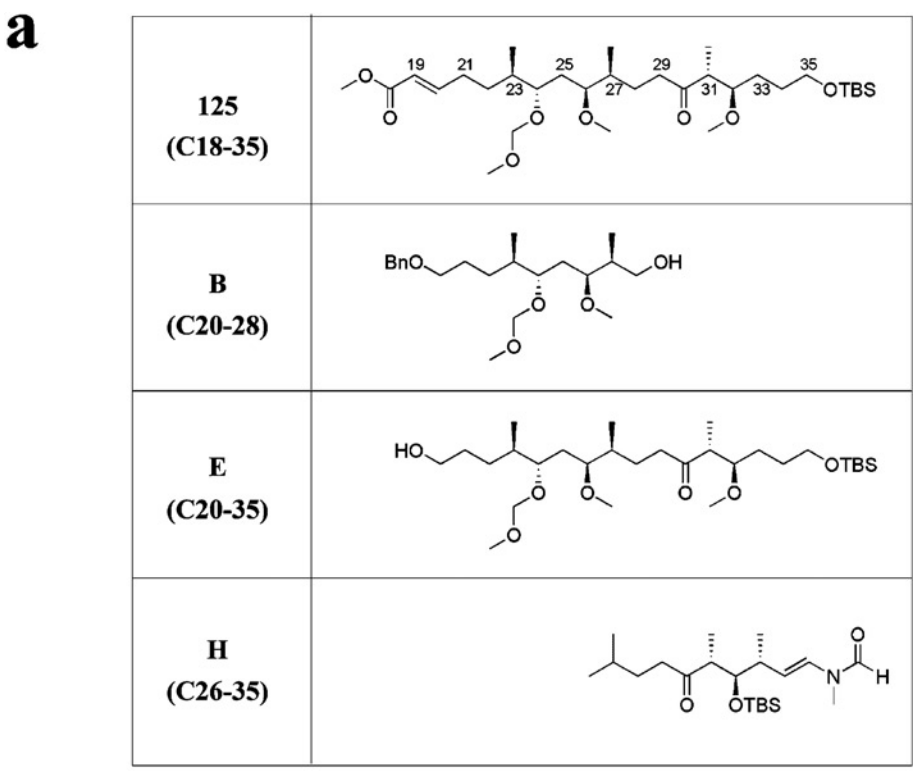

Figure 6. Halichondramide tail sub-fragments do not block SRF-dependent reporter gene expression. (*a*) Structures of halichondramide fragments. (125: C18–35) (*E*)-(6*R*,7*S*,9*S*,10*S*,14*R*,15*R*)-18-(*tert*-butyl-dimethyl-silanyloxy)-9,15-dimethoxy-7-methoxy-methoxy-6,10,14-trimethyl-13-oxo-octadec-2-enoic acid methyl ester; (B: C20–28) (2*S*,3*S*,5*S*,6*R*)-9-benzyloxy-3-methoxy-5-methoxymethoxy-2,6-dimethyl-nonan-1-ol; (E: C20–35) (4*R*,5*R*,9*S*,10*S*,12*S*,13*R*)-1-(*tert*-butyl-dimethyl-silanyloxy)-16-hydroxy-4,10-dimethoxy-12-methoxymethoxy-5,9,13-trimethyl-hexadecan-6-one; (H: C26–35) *N*-[(*E*)-(3*R*,4*R*,5*R*)-4-(*tert*-butyl-dimethyl-silanyloxy)-3,5,9-trimethyl-6-oxo-dec-1-enyl]-*N*-methyl-formamide. (*b*) HEK293 cells transfected with a SRE-luciferase reporter, a control β-galactosidase plasmid and an expression plasmid for active RhoA were incubated in medium with low serum for 24 h without compound or with 1 μM LatB, 10 μM 125, 10 μM B (C20–28), 10 μM E (C20–35) or 10 μM H (C26–35) as indicated. The data derive from four independent experiments in which compounds B, E and H were tested three times in duplicate; error bars show SD (n=3).

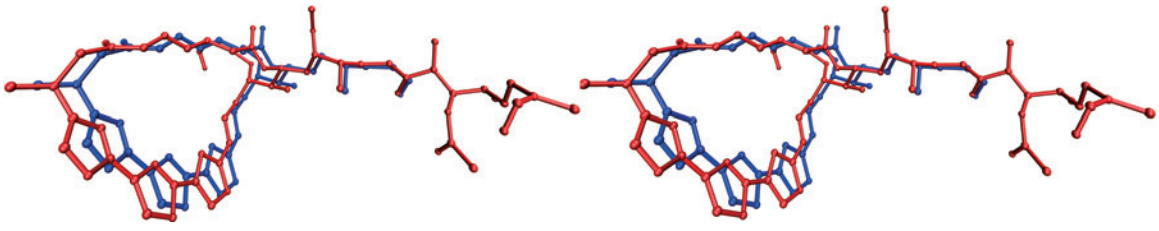

Figure 7. Computational model of ulapualide A. The stereo representation of the computational model (red) is overlaid with the crystallographic structure from the complex with actin (blue).

Table 1. Rigid docking of ulapualide A structures to actin

Fragment	Binding energy at ulapualide binding site (kcal mol^{-1})	Other lowest energy binding site?	Lowest energy site energy (kcal mol^{-1})
UlaA	–14.0	No	N/A
CYCLE	–10.7	No	N/A
TRIS	–7.1	Yes	–8.4
125	–9.4	No	N/A
E	–8.2	Yes	–9.6
B	–5.2	Yes	–10.5
H	N/A	Yes	–9.6

rithm, a single low energy binding site for ulapualide A was identified (see Table 1) with an rmsd of 1.3 Å compared to the crystallographic structure (Fig. 7). Similarly, a single site was also predicted for CYCLE, but not for the trisoxazole moiety alone (TRIS), suggesting that the intact heterocyclic ring may interact stably with G-actin. Most notably, a single low energy binding site was also predicted for 125 and this docking specificity was lost with the shorter tail compounds B, E and H, again consistent with experimental observation (Fig. 6). These findings are consistent with the notion that the experimental effects of 125 on SRF-dependent gene expression are due to G-actin binding.

Discussion

The ability to disrupt actin dynamics underlies the potent cytotoxicity of trisoxazole-based marine macrolides and qualifies these toxins as lead compounds for potential anti-metastatic drugs. Here we have compared the efficacy of the synthetic diastereoisomer of ulapualide A with that of the natural compound and found it to be three orders of magnitude lower. Furthermore, we have shown that a range of synthetic molecules corresponding to macrolide fragments all lack F-actin depolymerising properties, but that the aliphatic tail of halichondramide inhibits SRF-dependent gene expression, implying that macrolide derivatives could be used to uncouple the regulation of gene expression from actin dynamics.

Weak activity of the synthetic diastereoisomer of ulapualide A. The crystal structure of the G-actin-ulapualide A complex unequivocally established the stereochemistry of natural ulapualide A and confirmed that the synthetic compound represented one of its diastereoisomers [15]. The assumption that it would lack biological activity was not entirely borne out by the data, as cell adhesion and actin cytoskeletal integrity were both impaired, albeit only at 100–1000-fold higher concentrations (Figs 2b, 3b and data not shown). It is possible that the reversed chirality of C3 and C22–C24 has only a minor influence on the curvature of the trisoxazole macrolide moiety (see Fig. 1) and docking of the macrolide ring can occur in the natural conformation, but if this were the case, insertion of the aliphatic tail between subdomains 1 and 3 would be restricted. Alternatively, residual activity may be due to interactions of the aliphatic tail with G-actin without prior docking of the trisoxazole macrolide ring. A possible explanation for the inhibition of SRF-dependent gene expression by 125 (C18–35) could be its direct interaction with G-actin, which would indicate that the trisoxazole unit is not the sole contributor to actin binding. However, the structure of 125 corresponds to halichondramide rather than ulapualide A and its stereochemistry through C23–26 is that of the natural toxin not the diastereoisomer. Resolution of these uncertainties awaits further binding and structural studies.

Functional predictions for macrolide analogues from docking studies. From the crystal structure of the G-actin-ulapualide A complex, the macrocyclic ring was predicted to provide a major interface with G-actin, associating with the same hydrophobic patch as kabiramide C and jaspisamide A [14], while the aliphatic tail portion beyond C31 appeared to be rotationally free within the complex, due to the acetyl side chain at C32 [15]. The flexible docking studies indicated that the macrocyclic ring (CYCLE) may bind to G-actin, suggesting it to be the most likely moiety of ulapualide A with biological activity towards G-actin. However, CYCLE lacked detectable activity in any of the assays used, in line with an earlier structure-function study on aplyronine A, a marine macrolide with a ring and tail structure but lacking a trisoxazole unit, in which the tail was shown to be essential for actin depolymerising activity [26].

The interaction of ulapualide A with actin and its mechanism of action are thought to mimic the binding and severing action of gelsolin, whereby the anchoring

function of gelsolin domain 2 is performed by the trisoxazole macrolide ring and the severing function of domain 1, which displaces the DNase-binding loop of one actin molecule from the cleft between sub-domains 1 and 3 on the adjacent molecule in F-actin, is served by the aliphatic tail [14, 16]. This suggests that binding of the isolated trisoxazole ring of ulapualide A to F-actin in cells may have remained undetected in our assays. Alternatively, these partial compounds may have been degraded in the course of the experiments. Synthesis of a 7-(4-aminomethyl-1*H*-1,2,3-triazol-1-yl) analogue of CYCLE [27] would allow the generation of an optical probe to test these possibilities.

Although the flexible binding studies computed a binding energy for 125 that was 1.3 kcal mol^{-1} higher than that obtained for CYCLE, this was the only low energy binding site found for 125. Moreover, this selectivity was lost with the shorter tail analogues E, B and H (Fig. 6a). To investigate the possible contribution of specific intermolecular interactions towards binding of 125 to G-actin, several derivatives of 125 were constructed computationally and docked to the binding site. In these hypothetical derivatives, the $–CH_2–CH_2–$OTBS protecting group was replaced by –CH=CH–NMeCHO (as in compound H). A different substitution pattern on the terminal nitrogen, $N(CHO)CH_2OH$, led to a more favourable computed binding energy. Reduction of the isolated carbonyl group (C30) in 125 to $–CH_2–$ did not affect the binding energy, suggesting that this keto group in the natural substrate may be a historical artefact of the biosynthetic pathway. However, the neighbouring methyl substituent on C31 is computed to contribute ~0.5 kcal mol^{-1} to the binding energy. Introduction of a methoxy substituent at C28 led to other lower energy binding sites, indicating some significance of the presumed enzymatic reduction of this site during biosynthesis. Dehydrogenation either side of the diether side chain was explored, as the increased rigidity might have entropically favoured binding, but this modification reduced the specificity of binding. Finally, modification of the stereochemistry of the substituents at C23, C24, C26 or C27 individually was computed to disfavour binding, in accord with experiment. Thus, computational approaches suggest that further studies on 125 (C18–35) binding to G-actin are warranted.

A model for gene inhibition by 125 involving SRF cofactor MAL/MKL-1. The absence of actin-capping and -severing capability by 125 (C18–35) was expected. Although its ability to complex with F-actin cannot be entirely ruled out, it seems unlikely because its defined binding site is occluded in F-actin and no alternative low energy site was predicted by the docking analysis (Table 1). Thus, the unanticipated inhibitory effect of 125 on SRF-dependent gene expression is unlikely to stem from an increase in the G-actin pool.

SRF-dependent gene activation is thought to correlate with the release of the SRF co-activator MAL/MKL-1 from cytoplasmic complexes with G-actin and subsequent nuclear accumulation [8, 28]. Swinholide A, a toxin that links non-physiological G-actin dimers [29], was shown to stimulate SRF-dependent gene expression, presumably by disrupting G-actin-MAL/MKL-1 complexes [8]. A similar effect was observed with cytochalasin D, whereas latrunculin B, which also induces F-actin depolymerisation [2], inhibited SRF-dependent gene expression, apparently by stabilising the G-actin-MAL/MKL-1 complex [8, 13].

A simple model analogous to that for latrunculin B, *i.e.*, stabilisation of the G-actin-MAL/MKL-1 complex, would explain the inhibitory effect of 125 on SRF-dependent gene expression. However, although our flexible binding studies indicate that 125 might bind to the cleft between sub-domains 1 and 3, it is important to note that no direct experimental evidence to support this inference is available at present. Preliminary experiments to test the effect of compound 125 on the G-actin-MAL/MKL-1 complex gave ambiguous results. Under these circumstances it is not possible to rule out the possibility that 125 affects SRF-dependent gene expression by an alternative mechanism. Further experiments to test details of this model are currently underway. Nonetheless, our data indicate that fragments of actin binding macrolides can serve to modulate SRF-dependent gene expression without disrupting actin dynamics.

Acknowledgements. We thank the late Professor P. J. Sheuer for a gift of natural ulapualide A and Tim Self for assistance with the confocal microscopy. We also thank James Melville for helpful discussions about the docking calculations and Peter Jones for comments on the manuscript. Part of this work was supported by grants to GP from Pfizer Ltd, AstraZeneca and the EPSRC.

1 Spector, I., Braet, F., Shochet, N. R. and Bubb, M. R. (1999) New anti-actin drugs in the study of the organization and function of the actin cytoskeleton. Microsc. Res. Tech. 41, 18–37.
2 Yeung, K. S. and Paterson, I. (2002) Actin-binding marine macrolides: total synthesis and biological importance. Angew. Chem. Int. Ed. Engl. 41, 4632–4653.
3 Cen, B., Selvaraj, A. and Prywes, R. (2004) Myocardin/MKL family of SRF coactivators: Key regulators of immediate early and muscle specific gene expression. J. Cell. Biochem. 93, 74–82.
4 dos Remedios, C. G., Chhabra, D., Kekic, M., Dedova, I. V., Tsubakhara, M., Berry, D. A. and Nosworth, N. J. (2003) Actin binding proteins: regulation of cytoskeletal microfilaments. Physiol. Rev. 83, 433–473.
5 Giganti, A. and Friederich, E. (2003) The actin cytoskeleton as a therapeutic target: state of the art and future directions. Prog. Cell Cycle Res. 5, 511–525.
6 Cen, B., Selvaraj, A., Burgess, R. C., Hitzler, J. K., Ma, Z.,

Morris, S. W. and Prywes, R. (2003) Megakaryoblastic leukemia 1, a potent transcriptional coactivator for serum response factor (SRF), is required for serum induction of SRF target genes. Mol. Cell. Biol. 23, 6597–6608.
7 Wang, D. Z., Li, S., Hockemeyer, D., Sutherland, L., Wang, Z., Schratt, G., Richardson, J. A., Nordheim, A. and Olson, E. N. (2002) Potentiation of serum response factor activity by a family of myocardin-related transcription factors. Proc. Natl. Acad. Sci. USA 99, 14855–14860.
8 Miralles, F., Posern, G., Zaromytidou, A. and Treisman, R. (2003) Actin dynamics control SRF activity by regulation of its coactivator MAL. Cell 113, 329–342.
9 Morton, W. M., Ayscough, K. R. and McLaughlin, P. J. (2000) Latrunculin alters the actin-monomer subunit interface to prevent polymerization. Nat. Cell Biol. 2, 376–378.
10 Bubb, M. R., Senderowicz, A. M., Sausville, E. A., Duncan, K. L. and Korn, E. D. (1994) Jasplakinolide, a cytotoxic natural product, induces actin polymerization and competitively inhibits the binding of phalloidin to F-actin. J. Biol. Chem. 269, 14869–14871.
11 Bubb, M. R., Spector, I., Bershadsky, A. D. and Korn, E. D. (1995) Swinholide A is a microfilament disrupting marine toxin that stabilizes actin dimers and severs actin filaments. J. Biol. Chem. 270, 3463–3466.
12 Goddette, D. W. and Frieden, C. (1986) Actin polymerization. The mechanism of action of cytochalasin D. J. Biol. Chem. 261, 15974–15980.
13 Sotiropoulos, A., Gineitis, D., Copeland, J. and Treisman, R. (1999) Signal-regulated activation of serum response factor is mediated by changes in actin dynamics. Cell 98, 159–169.
14 Klenchin, V. A., Allingham, J. S., King, R., Tanaka, J., Marriott, G. and Rayment, I. (2003) Trisoxazole macrolide toxins mimic the binding of actin-capping proteins to actin. Nat. Struct. Biol. 10, 1058–1063.
15 Allingham, J. S., Tanaka, J., Marriott, G. and Rayment, I. (2004) Absolute stereochemistry of ulapualide A. Org. Lett. 6, 597–599.
16 Tanaka, J., Yan, Y., Choi, J., Bai, J., Klenchin, V. A., Rayment, I. and Marriott, G. (2003) Biomolecular mimicry in the actin cytoskeleton: Mechanisms underlying the cytotoxicity of kabiramide C and related macrolides. Proc. Natl. Acad. Sci. USA 100, 13851–13856.
17 Chattopadhyay, S. K. and Pattenden, G. (1998) Total synthesis of ulapualide A, a novel trisoxazole containing macrolide from the marine nudibranch *Hexabranchus sanguineus*. Tetrahedron Lett. 39, 6095–6098.
18 Chattopadhyay, S. K. and Pattenden, G. (2000) A total synthesis of the unique tris-oxazole macrolide ulapualide A produced by the marine nudibranch *Hexabranchus sanguineus*. J Chem. Soc. Perkin Trans 1, 2429–2454.
19 Frost, J. A., Steen, H., Shapiro, P., Lewis, T., Ahn, N., Shaw, P. E. and Cobb, M. H. (1997) Cross-cascade activation of ERKs and ternary complex factors by Rho family proteins. EMBO J, 16, 6426–6438.
20 Boussif, O., Lezoualc'h, F., Zanta, M. A., Mergny, M. D., Scherman, D., Demeneix, B. and Behr, J. P. (1995) A versatile vector for gene and oligonucleotide transfer into cells in culture and *in vivo*: polyethylenimine. Proc. Natl. Acad. Sci. USA 92, 7297–7301.
21 Pope, B. and Weeds, A. G. (1986) Binding of pig plasma gelsolin to F-actin and partial fractionation into calcium-dependent and calcium-independent forms. Eur. J. Biochem. 161, 85–93.
22 Morris, G. M., Goodsell, D. S., Halliday, R. S., Huey, R., Hart, W. E., Belew, R. K. and Olson, A. J. (1998) Automated docking using a Lamarckian genetic algorithm and empirical binding free energy function. J. Comput. Chem. 19, 1639–1662.
23 Hill, C. S., Wynne, J. and Treisman, R. (1995) The Rho family GTPasses RhoA, Rac1 and CDC42Hs regulate transcriptional activation by SRF. Cell 81, 1159–1170.
24 Shaw, P. E. and Saxton, J. (2003) Ternary complex factors: Prime nuclear targets for mitogen-activated protein kinases. Int. J. Biochem. Cell Biol. 35, 1210–1226.
25 Wang, D. Z. and Olson, E. N. (2004) Control of smooth muscle development by the myocardin family of transcriptional coactivators. Curr. Opin. Genet. Dev. 14, 558–566.
26 Kigoshi, H., Suenaga, K., Takagi, M., Akao, A., Kanematsu, K., Kamei, N., Okugawa, Y. and Yamada, K. (2002) Cytotoxicity and actin-depolymerizing activity of aplyronine A, a potent antitumor macrolide of marine origin, and its analogs. Tetrahedron 58, 1075–1102.
27 Petchprayoon, C., Suwanborirux, K., Miller, R., Sakata, T. and Marriott, G. (2005) Synthesis and characterization of the 7-(4-aminomethyl-1H-1,2,3-triazol-1-yl) analogue of kabiramide C. J. Nat. Prod. 68, 157–161.
28 Posern, G., Miralles, F., Guettler, S. and Treisman, R. (2004) Mutant actins that stabilise F-actin use distinct mechanisms to activate the SRF coactivator MAL. EMBO J. 23, 3973–3983.
29 Klenchin, V. A., King, R., Tanaka, J., Marriott, G. and Rayment, I. (2005) Structural basis of swinholide A binding to actin. Chem. Biol. 12, 287–291.